

Excitation function measurements for $^{12}\text{C}+^{12}\text{C}$ inelastic scattering channels

C. A. Bremner, S. P. G. Chappell, W. D. M. Rae, and I. Boztosun*

*Nuclear and Astrophysics Laboratory, University of Oxford, Keble Road, Oxford OX1 3RH, United Kingdom*M. Freer,[†] M. P. Nicoli, and S. M. Singer*School of Physics and Space Research, University of Birmingham, Edgbaston, Birmingham B15 2TT, United Kingdom*

B. R. Fulton, D. L. Watson, B. J. Greenhalgh, G. K. Dillon, and R. L. Cowin

Department of Physics, University of York, Heslington, York YO10 5DD, United Kingdom

(Received 13 May 2002; published 6 September 2002)

New experimental data for the $^{12}\text{C}+^{12}\text{C}$ reaction have been measured in the center-of-mass energy range $E_{\text{c.m.}}=40\text{--}59$ MeV. Excitation functions for a number of single and mutual ^{12}C inelastic channels have been measured which include the $0_{\text{g.s.}}^+$, 2_1^+ , 0_2^+ , 3_1^- , and 4_1^+ ^{12}C states. All of the reactions display largely unstructured excitation functions over this energy range. The absence of further resonances in this energy region for the $^{12}\text{C}(^{12}\text{C}, ^{12}\text{C}[3_1^-])^{12}\text{C}[3_1^-]$ reaction confirms theoretical predictions of the termination of the band of resonances found at lower center-of-mass energies in this channel.

DOI: 10.1103/PhysRevC.66.034605

PACS number(s): 25.70.Ef, 21.60.Gx, 27.30.+t, 27.20.+n

I. INTRODUCTION

Heavy-ion resonance reactions have been studied extensively over the past few decades. In particular the $^{12}\text{C}+^{12}\text{C}$ reaction has drawn significant interest. At low collision energies, close to the Coulomb barrier, resonances are observed in elastic and reaction channels, particularly $^{12}\text{C}(^{12}\text{C}, \alpha)^{20}\text{Ne}$ (see Ref. [1], and references therein). These resonances have widths of ~ 100 keV, characteristic of a lifetime approximately 10 times the collision time. The energy-spin systematics observe the $J(J+1)$ characteristic trend of a rotational system, and from the extracted rotational gradient ($\hbar^2/2I$) it is possible to infer a static deformation, which is found to be consistent with a $^{12}\text{C}+^{12}\text{C}$ cluster state, or molecule. At higher center-of-mass energies the widths of the resonances are characteristically larger (\sim MeV) and have been largely observed in inelastic channels. A large number of resonances have been found in, for example, inelastic reactions including the population of the 2_1^+ , 0_2^+ , 3_1^- , and 4_1^+ ^{12}C states [2–14]. It has been speculated that these broad resonances may be traced to either rotational structures [15,16], coupling of the elastic scattering channel to the inelastic channel via the crossing of aligned molecular bands (the band crossing model) [17–19], or interference effects resulting from reflected and refracted waves within the nuclear medium [7,20].

The inelastic resonances generally have common characteristics and are typified by the measurements of the single and mutual inelastic scattering to the first 2^+ state [4,5,7]. At $E_{\text{c.m.}}=10$ MeV the excitation functions reveal a series of narrow peaks which become increasingly broad, until they disappear at $E_{\text{c.m.}}\approx 45$ MeV. It has been observed [7] that this suppression of the resonance yield coincides with the

saturation of the fusion cross section. This saturation is believed to occur at the critical angular momentum of $L_c=19\pm 1\hbar$. Interestingly, a recent measurement of the $^{12}\text{C}(3^-)+^{12}\text{C}(3^-)$ reaction channel, in which alpha-particle unbound states are populated [12], found strong resonances extending up to $E_{\text{c.m.}}=43$ MeV, close to the point at which resonances terminate in the $^{12}\text{C}(^{12}\text{C}, ^{12}\text{C}[2^+])^{12}\text{C}[2^+]$ reaction. However, angular correlation analysis demonstrated that the spin of this highest energy resonance was $J=22\hbar$, three units larger than the critical angular momentum for fusion.

At present it is unknown if the resonance structures observed in the mutual 3^- inelastic channel persist to higher energies, and furthermore, if other highly inelastic channels involving the mutual population of states well above the α -decay threshold display resonance phenomena beyond the energy at which the broad resonances are observed in the $^{12}\text{C}(^{12}\text{C}, ^{12}\text{C}[2^+])^{12}\text{C}[2^+]$ reaction. The present study therefore extends the measurements of the excitation functions of the inelastic scattering to α -unbound states in the $^{12}\text{C}+^{12}\text{C}$ center-of-mass interval 40–59 MeV.

II. EXPERIMENTAL DETAILS

The present measurement was performed at the Australian National University (ANU). An experiment was conducted using the new Charissa strip detector array located in the MEGHA chamber [21]. For the present measurement the array was composed of eight $500\ \mu\text{m}$, $50\times 50\ \text{mm}^2$ Si strip detectors. These covered an angular range of $\theta_{\text{lab}}=5\text{--}60^\circ$, and an azimuthal angular range $\Delta\phi\approx 100^\circ$ each side of the beam axis, as shown in Fig. 1. Each strip detector was divided into 16 position-sensitive strips, providing very high segmentation, and the possibility of measuring emission angles and thus momenta with the high precision required for the reconstruction of the reaction kinematics. ^{12}C beams of 50 nA intensity ranging from $E_{\text{beam}}=80$ to 118 MeV were incident upon a $60\ \mu\text{g cm}^{-2}$ ^{12}C foil target, producing a data event rate of 5 kHz. The target thickness was found to in-

*Present address: Department of Physics, Erciyes University, 38039 Kayseri, Turkey.

[†]Corresponding author. Email address: M.Freer@bham.ac.uk

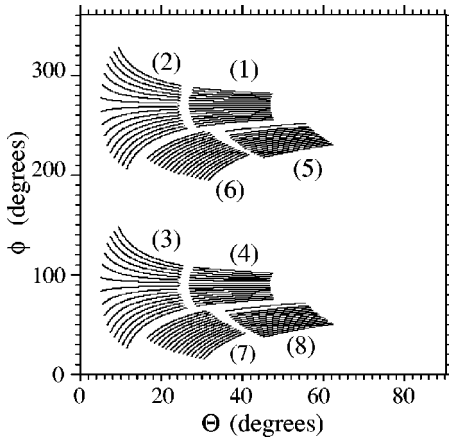


FIG. 1. The arrangement of the strip detectors used in the present measurement. Note the beam axis is located at the midpoint between detectors 2 and 3. The plot shows the experimental acceptance of the eight detectors in spherical polar coordinates.

crease by 25% during the run which was corrected for in the analysis of the reaction yields. The higher energies ($E > 99$ MeV) were obtained using the linear accelerator in conjunction with the pelletron tandem 14UD accelerator. Due to the high beam energies used and the limited detector thickness, events involving α particles, with an energy in excess of ~ 32 MeV, experienced punch-through (i.e., the particles did not stop in the silicon detectors) and thus only a fraction of the α -particle energy was deposited in the detector. A Monte Carlo simulation of the reaction and detection processes indicated that only 4.8% of events at the highest beam energy experience punch-through for the mutual $^{12}\text{C}(3_1^-)$ channel. This fraction is much higher for the other dominant channels, and particularly for those involving the $^{12}\text{C}(4_1^+)$ state. Such processes contribute to the overall background levels observed at the higher energies. However, the reconstruction methods employed in the analysis were able to clearly distinguish the punch-through events, suppressing this contribution. The loss of acceptance was accounted for using the Monte Carlo simulations.

III. ANALYSIS AND RESULTS

The experimental trigger requirement was a total strip multiplicity of greater than three; this implies that the measurement is only sensitive to inelastic channels in which one of the ^{12}C nuclei was excited into an α -unbound state. Since the α decay of ^{12}C feeds states in ^8Be , all of which are unbound to α decay, a three- α final state results. Such a decay process occurs for all but the ^{12}C ground state and 4.4 MeV (2_1^+) states. Thus, for inelastic channels involving a ^{12}C nucleus in one of these bound states and the other ^{12}C in an unbound state the final multiplicity will be four. If, however, both ^{12}C nuclei are excited to α -decaying states then the final state multiplicity is then six. The detection of only five of the six final state particles is sufficient to fully reconstruct the reaction kinematics. Further details of the reconstruction techniques can be found in Refs. [11,12,22,23].

The α -decay process is such that the three α particles are

emitted into a cone with an opening angle which is small compared with the detector geometry. Thus if three hits are observed on one side of the beam axis there is a large probability that they arise from the decay of ^{12}C .

It should be noted that there was no explicit particle identification in these measurements, however the reaction kinematics may in fact be used to identify unique reaction products and decay channels. For example, the reconstruction of the excitation energy of the parent ^{12}C nuclei from the momenta of the three α particles should identify which state was excited in the reaction process. Such a spectrum is plotted in Fig. 2 for a final state consisting of six α particles, where the excitation energy for both ^{12}C nuclei produced in the collision is reconstructed. The two dimensional spectrum reveals the mutual excitations of the ^{12}C nuclei, and the excitation energies of the states are indicated on the projections. The dominant states in these spectra are the 0_2^+ (7.6542 MeV), 3_1^- (9.641 MeV), and 4_1^+ (14.083 MeV) states. It is also possible to reconstruct the decay path for the ^{12}C α decay, i.e., via the ^8Be ground state or ^8Be 3.04 MeV (2^+) state. Also shown in Fig. 2 is the decomposition of the excitation spectrum between these possible decay branches. As expected, the decay of the 4_1^+ state proceeds predominantly via the ^8Be excited state, while the decay of the 0_2^+ and 3_1^- states feeds the ^8Be ground state. By placing two dimensional gates on the spectrum in Fig. 2 it is possible to isolate the various mutual excitations, and thus to extract the energy dependence of the various reaction yields. Experimental yields were determined by performing a Gaussian fit, including a linear background term, to the projections. The results of this analysis are shown in Figs. 3–6.

IV. DISCUSSION

Figure 3 shows the previously measured mutual $^{12}\text{C}(3_1^-)$ excitation function [12]. In the original work these data were not normalized for the detector efficiency or the target thickness, but are just normalized to the integrated beam exposure. In order to compare the present measurements with those shown in Fig. 3, we have analyzed the mutual $^{12}\text{C}(3_1^-)$ yields by placing software cuts around an angular region which coincide with that of the previous measurements [12]. The resulting excitation function has then been scaled by the ratio of the nominal target thickness in the two measurements (100:60). Given that the calculated detection efficiencies are very similar over the region of overlap, no correction has been made for this factor. It is clear that the two measurements agree reasonably well. There is a slight discrepancy in the overall magnitude of the cross sections of $\sim 10\%$ but this is within the uncertainties of the two target thicknesses. The data do not extend to low enough energies to observe the decrease in yield towards $E_{c.m.} = 40$ MeV, however the decrease in yield towards $E_{c.m.} = 45$ MeV is well reproduced. There is one notable discrepancy, and that is the failure of the present measurement to find the sharp increase in yield at $E_{c.m.} = 43$ MeV. Since the two measurements used different target thicknesses, they sample slightly different center-of-mass energy intervals. In the present case the 60

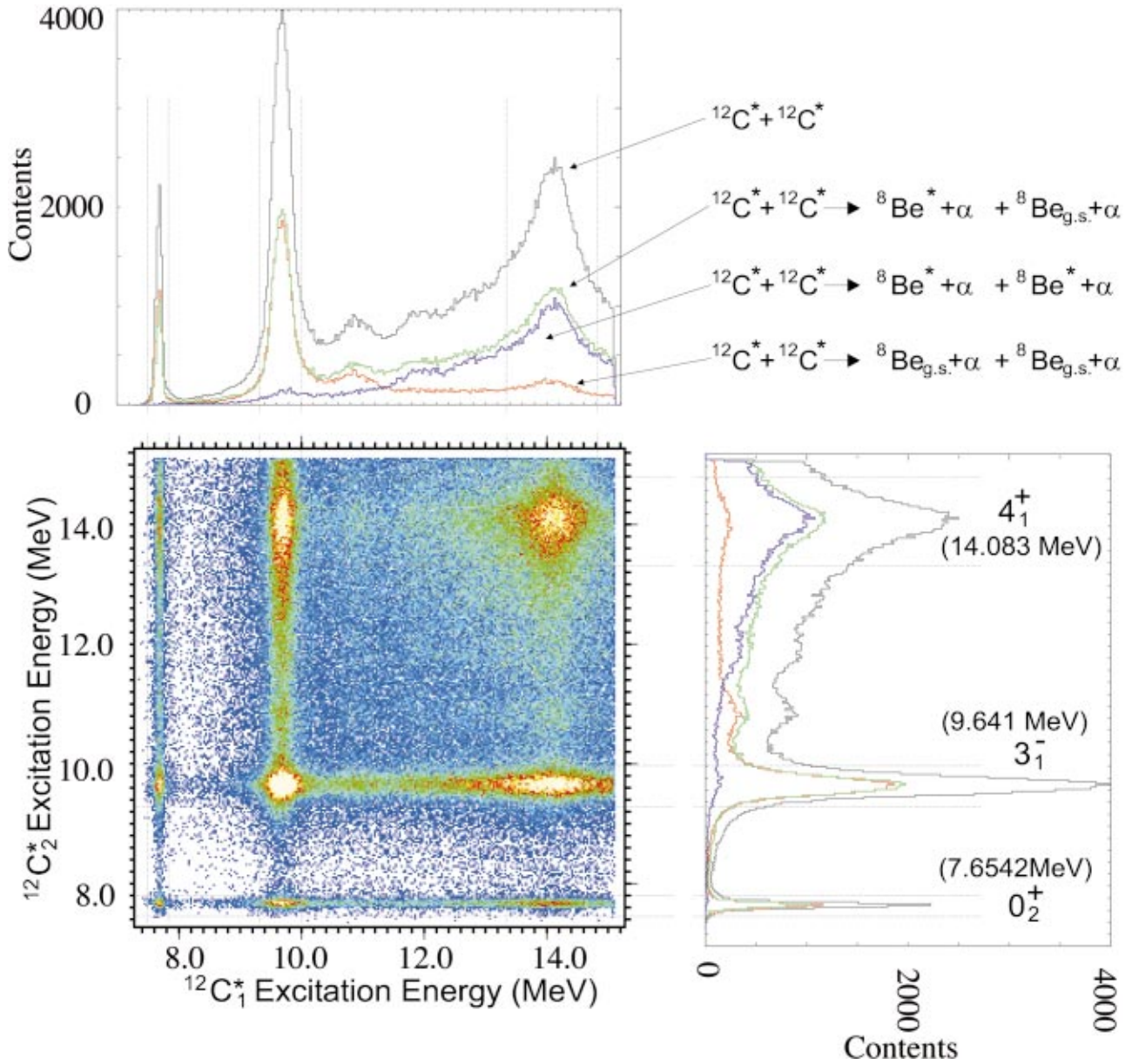


FIG. 2. (Color) The reconstructed ^{12}C excitation energies for sixfold $^{12}\text{C}^* + ^{12}\text{C}^*$ events at the highest beam energy. The one dimensional projections indicate excitation energies of the states observed in the reaction. The strength of the decay of each state via either the ^8Be ground state or first excited state is indicated by the ancillary lines on the one dimensional spectra. Also indicated on the two dimensional spectrum are the gates used to filter the data (horizontal and vertical dotted lines).

$\mu\text{g cm}^{-2}$ target produced an energy averaging in the center-of-mass frame of 50 keV, whereas the thicker $100 \mu\text{g cm}^{-2}$ target produced a spread of 80 keV. Alternatively, it is possible that the beam energies produced by the 14UD did not coincide exactly for the two measurements. Measurements of the reproducibility of the energy of the 14UD suggest that the uncertainty could be as large as 0.2% [24], which in this instance would correspond to ~ 90 keV in the center of mass. If either of these possibilities were the case, it would suggest that the sharp peak at $E_{\text{c.m.}} = 43$ MeV might comprise narrow structures ($\Gamma_{\text{c.m.}} < 100$ keV). This intriguing possibility would require further investigation via thin target measurements and with much finer center-of-mass energy steps.

It is clear that no further resonances are observed in the

extended energy range, but only a smooth attenuation of the reaction yield. The Monte Carlo calculations, which use isotropic angular distributions, show that the detection efficiency is approximately constant as a function of center-of-mass energy, and thus the decrease in the reaction yield cannot be explained by decreasing acceptances. Thus, we believe that this result shows the termination of the structures associated with the 3_1^- resonances at $E_{\text{c.m.}} = 43$ MeV.

Figures 4–6 show the excitation functions for the various reaction channels which have been observed in the present measurement for the full experimental acceptance. These figures show the experimental cross sections deduced from the normalization to the integrated beam current, and from calculations of the detection efficiency evaluated as a function

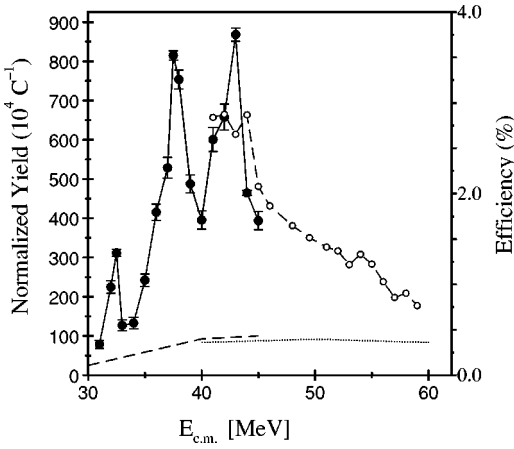


FIG. 3. Experimental excitation functions for the $^{12}\text{C}(^{12}\text{C}, ^{12}\text{C}[3_1^-])^{12}\text{C}[3_1^-]$ channel. Results are shown for a comparison with the previous data of Chappell *et al.* (Ref. [12]) with the present data. Also indicated is the Monte Carlo simulation for the detection efficiencies for each of the experimental data sets. See the text for details of the normalization.

of the center-of-mass energy. These efficiencies are shown for reference in Fig. 7, and were again calculated using isotropic angular distributions. We note that the cross sections calculated here are in good agreement with earlier measurements [6,9], where overlap of energy regions between data

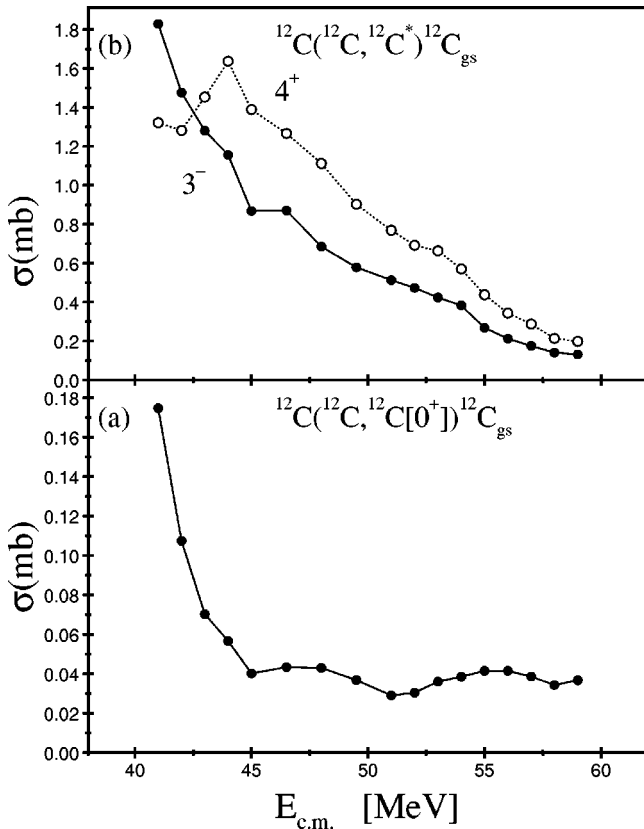


FIG. 4. Experimental excitation functions for the (a) $^{12}\text{C}(^{12}\text{C}, ^{12}\text{C}[0_2^+])^{12}\text{C}_{\text{g.s.}}$ reaction, and (b) for the $^{12}\text{C}(^{12}\text{C}, ^{12}\text{C}[3_1^-, 4_1^+])^{12}\text{C}_{\text{g.s.}}$ reactions.

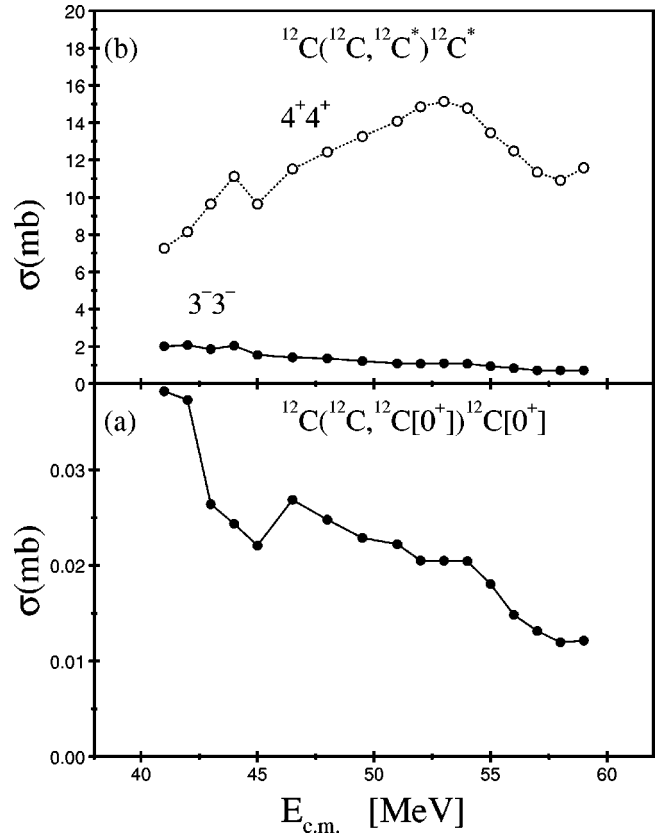


FIG. 5. Experimental excitation functions for the (a) $^{12}\text{C}(^{12}\text{C}, ^{12}\text{C}[0_2^+])^{12}\text{C}[0_2^+]$ and (b) $^{12}\text{C}(^{12}\text{C}, ^{12}\text{C}[4_1^+])^{12}\text{C}[4_1^+]$, $^{12}\text{C}(^{12}\text{C}, ^{12}\text{C}[3_1^-])^{12}\text{C}[3_1^-]$ reactions.

sets allows comparison, and that in all instances the statistical errors are smaller than the data symbols. Figures 4 and 5 show the ^{12}C single and mutual excitations, respectively, involving the 0_2^+ , 3_1^- , and 4_1^+ channels. It is clear that none of the channels involving the 0_2^+ , 3_1^- , and 4_1^+ states possess the type of resonant structure that is present at lower energies in the $^{12}\text{C}(3_1^-) + ^{12}\text{C}(3_1^-)$ or other inelastic channels. The $^{12}\text{C}_{\text{g.s.}} + ^{12}\text{C}^*$ reactions generally show a steady decrease in strength with increasing energy. The increase in yield as the energy decreases towards $E_{\text{c.m.}} = 44$ MeV is consistent with earlier measurements of these reactions [25] where a resonance was observed in the $^{12}\text{C}_{\text{g.s.}} + ^{12}\text{C}(3_1^-)$ and $^{12}\text{C}_{\text{g.s.}} + ^{12}\text{C}(0_2^+)$ reactions at $E_{\text{c.m.}} = 41$ MeV. There is perhaps some evidence for a small enhancement in the cross section in the $^{12}\text{C}_{\text{g.s.}} + ^{12}\text{C}(4_1^+)$ reaction also close to $E_{\text{c.m.}} = 44$ MeV. Enhancements are also observed in the $^{12}\text{C}(3_1^-) + ^{12}\text{C}(3_1^-)$ and $^{12}\text{C}(4_1^+) + ^{12}\text{C}(4_1^+)$ mutual excitations, shown in Fig. 5(b), at the same energy. This is close to the large peak previously observed in the $^{12}\text{C}(3_1^-) + ^{12}\text{C}(3_1^-)$ reaction [25] at $E_{\text{c.m.}} = 43$ MeV.

Figure 6 presents the remaining mutual channels which have significant yield in this energy range. Again, although broad structures are present, there is no evidence that strong resonances have been observed. There is some indication of enhancements at $E_{\text{c.m.}} = 44$ MeV in the $^{12}\text{C}(2_1^+) + ^{12}\text{C}(3_1^-)$, $^{12}\text{C}(4_1^+) + ^{12}\text{C}(3_1^-)$, $^{12}\text{C}(0_2^+) + ^{12}\text{C}(3_1^-)$, and $^{12}\text{C}(0_2^+)$

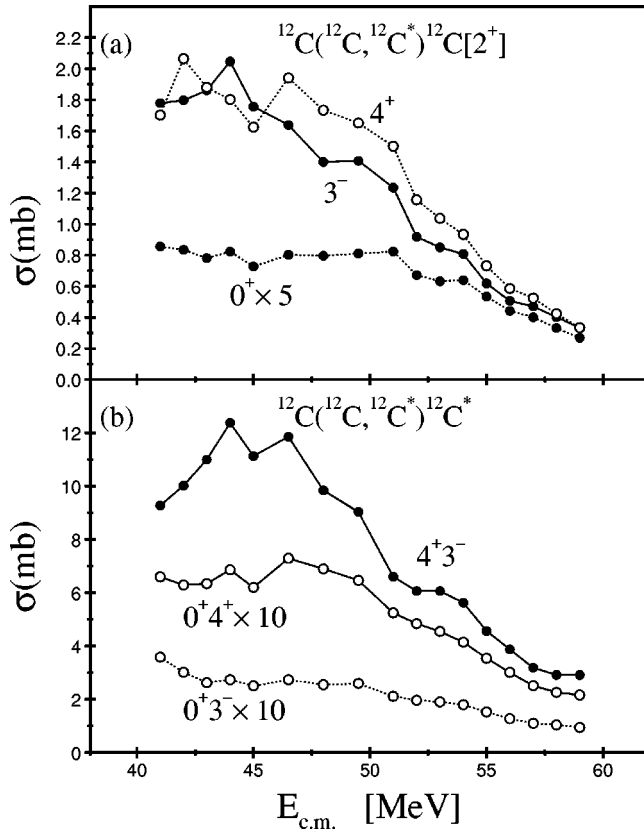


FIG. 6. Experimental excitation functions for the (a) $^{12}\text{C}(2_1^+) + ^{12}\text{C}^*$ reactions, and (b) the $^{12}\text{C}(0_2^+) + ^{12}\text{C}(3_1^-)$, $^{12}\text{C}(0_2^+) + ^{12}\text{C}(4_1^+)$, and $^{12}\text{C}(3_1^-) + ^{12}\text{C}(4_1^+)$ reactions.

+ $^{12}\text{C}(4_1^+)$ reactions, and the $^{12}\text{C}(3_1^-) + ^{12}\text{C}(4_1^+)$ channel shows weak evidence for a further structure at $E_{\text{c.m.}} = 46$ MeV. But, in general all of the reaction channels demonstrate a rather smooth energy dependence over the measured energy range.

Thus, the present measurements find little evidence for strong broad ($\Gamma > 500$ keV) resonant structures in the energy interval $E_{\text{c.m.}} = 45\text{--}59$ MeV. Moreover, in the description of the resonances in terms of a common rotational band, the structure in the $3_1^- + 3_1^-$ channel at $E_{\text{c.m.}} = 43$ MeV, which Chappell *et al.* [12] identified as $J = 22\hbar$ would appear to be the terminating state. We note that the cranked alpha-cluster model (ACM) [15], Hartree-Fock (HF) calculations [16], and Nilsson-Strutinsky (NS) calculations [26,27] predict a number of rotational bands whose energy-spin characteristics may be tested against experimental data. These calculations suggest the planar-cluster structure with a large overlap with two oblate ^{12}C nuclei with their deformation axes aligned (the so-called F1 configuration [16,15]) has a rotational band which terminates at $J = 20\text{--}24\hbar$, depending on the details of the model, which is consistent with the $J = 22\hbar$ assignment of Chappell *et al.* It is possible, given that the energy-spin systematics of the calculations also reproduce those of the experimental data, that the resonances observed in the $3_1^- + 3_1^-$ channel correspond to the F1 configuration.

However, the termination of structure in all of the observed reaction channels at an energy coincident with the

saturation of the fusion cross section is curious. This has been interpreted in terms of the trapping of the two ^{12}C nuclei in a pocket in the inter-ion potential, which no longer exists when the angular momentum reaches $19\hbar$ [7]. It is possible that this description coincides with the above interpretation in terms of a rotational band associated with the triaxial F1 configuration. The termination of the rotational band would correspond to the disappearance of a minimum in the ACM, HF, and NS calculations. However, the results of Chappell *et al.* [12] indicate that this does not occur until $J = 22\hbar$.

The band crossing model (BCM) describes the appearance of resonances in such reactions in terms of the coupling of flux from the elastic to inelastic channel via the crossing of aligned molecular bands [17–19]. The BCM in general is able to account for the energies and spins of resonances observed, for example, in the $^{12}\text{C}(^{12}\text{C}, ^{12}\text{C}[2^+])^{12}\text{C}[2^+]$ reaction [19]. In this description empirical potentials were used to describe the interactions. More recently, potentials derived from double-folding calculations have been used successfully in the coupled channels formalism to calculate the cross sections for inelastic channels leading to the population of α -unbound states in ^{12}C [28–30]. These calculations provide a very reasonable description of the experimental data, but over quite a limited energy range. There is a direct link between such coupled channels calculations and the coupling of reaction channels in the BCM; this connection is discussed in detail, for example, in Ref. [29]. The coupled channels calculations performed to date successfully reproduce the evolution from narrow resonances at low center-of-mass energies to the much broader structures seen at higher energy [28,30], thus the observation of a broad structure in several of the reaction channels at $E_{\text{c.m.}} = 44$ MeV is consistent with such a description.

It is clear that over the center-of-mass energy range $E_{\text{c.m.}} = 40\text{--}59$ MeV that the inelastic reactions involving the population of α -particle unbound states are dominated by those which include the excitation of the 14.083 MeV (4^+) state. Thus, coupled channel calculations which attempt to reproduce the energy dependence of the inelastic scattering over this energy region must include the coupling to this state. Previous calculations have focused on coupling either to only the 2^+ state, e.g., Refs. [29,31], or have not been extended to the present energies. The combination of experimental excitation functions for a very large number of reaction channels over a wide energy interval, together with the experimentally determined angular momenta associated with the various resonances should now provide a stringent test of the coupled channels approach.

V. SUMMARY AND CONCLUSIONS

The present study provides excitation function measurements for the dominant single and mutual ^{12}C inelastic reaction channels leading to particle unbound states in the energy range $E_{\text{c.m.}} = 40\text{--}59$ MeV. On the whole these reactions appear to possess a smooth energy dependence, and lack of distinct structures in the excitation functions above $E_{\text{c.m.}} = 45$ MeV indicates that resonant processes do not domi-

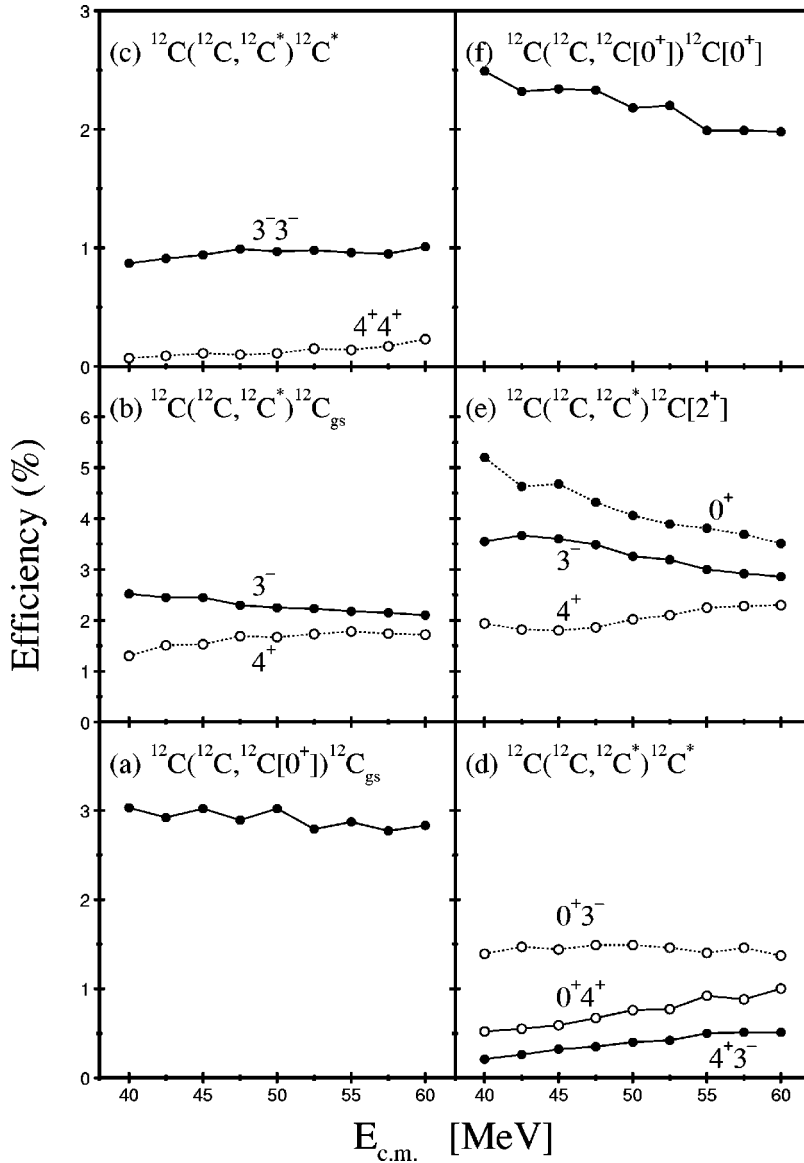


FIG. 7. The calculated detection efficiencies used in the calculation of the cross sections in Figs. 4–6. These calculations include the punch-through effect described in the text. Note the same symbols have been used for both the efficiency calculation and the experimental cross sections.

nate. The lack of resonances in the higher energy interval is consistent with the observations made for the inelastic channels $^{12}\text{C}(2^+) + ^{12}\text{C}(2^+)$ and $^{12}\text{C}_{\text{g.s.}} + ^{12}\text{C}(2^+)$, where the termination has been linked with the disappearance of a pocket in the inter-ion potential. Given the observed termination of the resonances in the $^{12}\text{C}(3_1^-) + ^{12}\text{C}(3_1^-)$ reaction we suggest that this pocket vanishes for angular momenta of $J \approx 22\hbar$.

In addition, these measurements indicate that over this energy range reactions involving the population of the 14.083 MeV (4^+) state are stronger than other inelastic scattering reactions involving the population of states above the ^{12}C α -decay threshold. These measurements should thus al-

low the prediction of resonance energies and spins produced from the scattering potential in the coupled channels approach to be further tested.

ACKNOWLEDGMENTS

The authors wish to thank the staff of the Department of Nuclear Physics at the Australian National University for assistance in running the experiments. We acknowledge the financial support of the U.K. Engineering and Physical Sciences Research Council (EPSRC). The experimental work was performed under a formal agreement between the EPSRC and ANU.

- [1] K. A. Erb and D. A. Bromley, in *Treatise on Heavy-Ion Science*, edited by D. A. Bromley (Plenum, New York, 1984), Chap. 3, Vol. 3, pp. 201–310.
 [2] N. Cindro, *Riv. Nuovo Cimento* **4**, 1 (1981).
 [3] N. Cindro, *Ann. Phys. (Paris)* **13**, 289 (1988).

- [4] T. M. Cormier, J. Applegate, G. M. Berkowitz, P. Braun-Munzinger, P. M. Cormier, J. W. Harris, C. M. Jachcinski, L. L. Lee, Jr., J. Barrette, and H. E. Wegner, *Phys. Rev. Lett.* **38**, 940 (1977).
 [5] T. M. Cormier, C. M. Jachcinski, G. M. Berkowitz, P. Braun-

- Munzinger, P. M. Cormier, M. Gai, J. W. Harris, J. Barrette, and H. E. Wegner, *Phys. Rev. Lett.* **40**, 924 (1978).
- [6] B. R. Fulton, T. M. Cormier, and B. J. Herman, *Phys. Rev. C* **21**, 198 (1980).
- [7] A. Morsad, F. Haas, C. Beck, and R. M. Freeman, *Z. Phys. A* **338**, 61 (1991).
- [8] A. H. Wuosmaa, R. R. Betts, M. Freer, B. G. Glagola, Th. Happ, D. J. Henderson, P. Wilt, and I. G. Beardon, *Phys. Rev. Lett.* **68**, 1295 (1992).
- [9] A. H. Wuosmaa, *Z. Phys. A* **349**, 249 (1994); A. H. Wuosmaa, M. Freer, B. B. Back, R. R. Betts, J. C. Gehring, B. G. Glagola, Th. Happ, D. J. Henderson, P. Wilt, and I. G. Bearden, *Phys. Rev. C* **50**, 2909 (1994).
- [10] S. P. G. Chappell, D. L. Watson, S. P. Fox, C. D. Jones, W. D. M. Rae, P. M. Simmons, M. Freer, B. R. Fulton, N. M. Clarke, N. Curtis, M. J. Leddy, J. S. Pople, S. J. Hall, R. P. Ward, G. Tungate, W. N. Catford, G. J. Gyapong, S. M. Singer, and P. H. Regan, *Phys. Rev. C* **51**, 695 (1995).
- [11] S. P. G. Chappell and W. D. M. Rae, *Phys. Rev. C* **53**, 2879 (1996).
- [12] S. P. G. Chappell, W. D. M. Rae, C. A. Bremner, G. K. Dillon, D. L. Watson, B. Greenhalgh, R. L. Cowin, M. Freer, and S. M. Singer, *Phys. Lett. B* **444**, 260 (1998).
- [13] R. A. Le Marechal, N. M. Clarke, M. Freer, B. R. Fulton, S. J. Hall, S. J. Hoad, G. R. Kelly, R. P. Ward, C. D. Jones, P. Lee, and D. L. Watson, *Phys. Rev. C* **55**, 1881 (1997).
- [14] S. Szilner, Z. Basrak, R. M. Freeman, F. Haas, A. Morsad, M. P. Nicoili, and C. Beck, *J. Phys. G* **25**, 1927 (1999).
- [15] S. Marsh and W. D. M. Rae, *Phys. Lett. B* **180**, 185 (1986).
- [16] H. Flocard, P. H. Heenen, S. J. Krieger, and M. S. Weiss, *Prog. Theor. Phys.* **72**, 1000 (1984).
- [17] Y. Kondo, Y. Abe, and T. Matsuse, *Phys. Rev. C* **19**, 1356 (1979).
- [18] Y. Abe, Y. Kondo, and T. Matsuse, *Prog. Theor. Phys. Suppl.* **68**, 303 (1980).
- [19] T. Matsuse, Y. Abe, and Y. Kondo, *Prog. Theor. Phys.* **59**, 1904 (1978).
- [20] N. Rowley, H. Doubre, and C. Marty, *Phys. Lett.* **69B**, 147 (1977).
- [21] R. L. Cowin and D. L. Watson, *Nucl. Instrum. Methods Phys. Res. A* **399**, 365 (1997).
- [22] T. Davinson, A. C. Shotter, E. W. Macdonald, S. V. Springham, P. Jobanputra, A. J. Stephens, and S. L. Thomas, *Nucl. Instrum. Methods Phys. Res. A* **288**, 245 (1990).
- [23] S. Shimoura, A. Aakaguchi, T. Shimoda, T. Fukuda, K. Ogura, and K. Katori, *Nucl. Phys.* **A452**, 123 (1986).
- [24] R. H. Spear, D. C. Kean, M. T. East, A. M. Joye, and M. P. Fewell, *Nucl. Instrum. Methods* **147**, 455 (1977).
- [25] S. P. G. Chappell, DPhil thesis, University of York, 1995.
- [26] G. Leander and S. E. Larsson, *Nucl. Phys.* **A239**, 93 (1975).
- [27] I. Ragnarsson, S. Aberg, and R. K. Sheline, *Phys. Scr.* **24**, 215 (1981).
- [28] Y. Hirabayashi, Y. Sakuragi, and Y. Abe, *Phys. Rev. Lett.* **74**, 4141 (1994).
- [29] M. Ito, Y. Sakuragi, and Y. Hirabayashi, *Phys. Rev. C* **63**, 064303 (2001).
- [30] Y. Sakuragi, M. Ito, M. Katsuma, M. Takashina, Y. Kudo, Y. Hirabayashi, S. Okabe, and Y. Abe, in *Proceedings of the Seventh International Conference on Clustering Aspects of Nuclear Structure and Dynamics*, edited by M. Korolija, Z. Basrak, and R. Caplar (World Scientific, Singapore, 2000), p. 138.
- [31] I. Boztosun and W. D. M. Rae, *Phys. Rev. C* **63**, 054607 (2001).